

## Crystallization Kinetics Study in Al<sub>87</sub>Ni<sub>10</sub>La<sub>3</sub> Amorphous Alloy

Amir Roofigar Haghighi<sup>1</sup>, Akbar Heidarpour<sup>1,\*</sup>, Mohsen Eshaghpour Soorani<sup>2</sup>, Mehdi Mansouri<sup>2</sup>

<sup>1</sup> Department of Metallurgy and Materials Engineering, Hamedan University of Technology, Hamedan, 65155-579, Iran.

<sup>2</sup> Materials Engineering Faculty, Islamic Azad University, Najafabad Branch, Isfahan, Iran.

---

### ARTICLE INFO

#### Article history:

Received 13 May 2018

Accepted 14 July 2018

Available online 5 November 2018

#### Keywords:

Amorphous alloy  
Rapid solidification  
Crystallization  
Thermal Analysis

---

### ABSTRACT

In this study, the crystallization behavior of melt-spun Al<sub>87</sub>Ni<sub>10</sub>La<sub>3</sub> amorphous phase was investigated by using X-ray diffraction and non-isothermal differential thermal analysis techniques. The results demonstrated that the amorphous phase exhibited two-stage crystallization on heating, i.e., at first step the amorphous phase transforms into  $\alpha$ -Al phase and at second step Al<sub>11</sub>La<sub>3</sub> and Al<sub>3</sub>Ni intermetallic phases precipitate, simultaneously. The activation energies of the crystallizations of the amorphous phase were evaluated by the Kissinger equation using the peak temperature of the exothermic reactions. The values of two-step crystallization activation energies were approximately 173.7±6 and 278.4±5 kJ/mol, respectively. The Avrami index was calculated for the first and second step of crystallizations and obtained 0.9 and 3.8 respectively. This kinetics investigation indicated that in the first step of crystallization of Al<sub>87</sub>Ni<sub>10</sub>La<sub>3</sub> alloy, the nucleation rate decreases with time, and the crystallization is governed by a three-dimensional diffusion-controlled growth, while the second stage was in interface control regime.

---

### 1-Introduction

Al-based alloys have low density and good corrosion resistance that make them a good candidate for the transportation and aviation industries [1, 2]. Among the Al-based alloys, amorphous alloys are a new class of them, which have received much attention recently [3-6] because these alloys are sufficiently adaptable, and they have an unusual combination of properties such as high strength, good ductility, and last but not least good corrosion resistance. It has been shown that these types of alloys can be prepared by using either rapid solidification or mechanical alloying (MA) techniques [7-11]. Among the various amorphous Al alloy systems, Al-Ni-RE (La, Y, Ce) amorphous alloys have

been studied intensively because of their excellent glass-forming ability (GFA) and high thermal stability [12-15]. It has been reported that the glass formation is favored in multicomponent compositions of these types of alloys [16-20]. In addition to the alloying development to produce amorphous Al alloy with higher GFA, several investigations also have focused on studying the crystallization process of amorphous Al-based alloys [21-27]. The controlled crystallization of these materials improves the properties and this issue is very attractive in many engineering applications. Generally, there are two basic approaches to determine kinetics parameters of amorphous alloys during heat treatment, which are

---

\* Corresponding author:

E-mail address: heidarpour@hut.ac.ir

isothermal and non-isothermal methods [28-30]. The isothermal experimental analysis techniques were in most cases more definitive and the well-known Johnson–Mehl–Avrami (JMA) kinetics equation was always assumed [31–36]. But the kinetics of a primary crystallization reaction was not easy to fit to any established model of phase transformations in contrast to polymorphous or eutectic crystallization. Meanwhile, it could be seen that the non-isothermal thermo-analytical techniques had several advantages. The rapidity with which non-isothermal experiments could be performed made these types of experiment attractive. Non-isothermal experiments could be used to extend the temperature range of measurements beyond that accessible to isothermal experiment. Also, many phase transformations occurred too rapidly to be measured under isothermal conditions because of their transients nature. Finally, industrial processes often depended on the kinetic behavior of systems undergoing phase transformations under non-isothermal conditions [29]. The study of the kinetics of crystallization provided the activation energy of crystallization and parameters like Avrami index, which responsible for the mechanism of crystallization. In this instance a definitive measurement of non-isothermal transformation kinetics was desirable.

The previous study [37] has shown that the crystallization of fcc-Al nanoparticles in amorphous  $\text{Al}_{90-x}\text{Ni}_{10}\text{MM}_x$  (MM: Ce rich mischmetal;  $x=2, 4$ ) alloys are a complex process. By thermal analysis, it has been found that the activation energy of crystallization (E) is changed with the continuation of the phase transformation, particularly at the late stage. This study proposed to study phase change during heating of amorphous  $\text{Al}_{87}\text{Ni}_{10}\text{La}_3$  alloy and to determine the activation energy of crystallization process, which describes the mechanism of the crystallization by employing

non-isothermal models. The results were compared to other researches.

## 2- Materials and methods

The alloy with a nominal composition of  $\text{Al}_{87}\text{Ni}_{10}\text{La}_3$  was prepared by vacuum induction melting of the mixture of pure Al (99.99 wt%), Ni (99.99 wt%) and La (99.99 wt.%) under a high purity Ar atmosphere in a quartz crucible. Melting was performed several times to ensure compositional homogeneity of the alloying elements in the ingot. Amorphous ribbons with a width of 2–3 mm and a thickness of 30  $\mu\text{m}$  were prepared by a single roll melt spinning machine. The tangential velocity and diameter of Cu wheel were 40 m/s and 200 mm respectively. The phase analysis of the ribbons, immediately after melt spinning, was performed by X-Ray diffraction (XRD) with  $\text{Cu K}\alpha$  radiation (AW-XDM 300, China). The simultaneous thermal analysis was performed up to 700°C at rates of 2.5-40°C/min under protective  $\text{N}_2$  atmosphere to analyze the crystallization behavior of sample during heat treatment in a thermal analysis instrument STA 449F3, NETZCH, Germany. In order to identify the phases after each exothermic peak in thermal analysis curve, the pieces of ribbons were heat treated isochronally (20 K/min) in STA instrument up to preset temperature and then cooled to room temperature. The kinetic studies are based on the ICTAC Kinetics Committee recommendations for collecting kinetic data [38] and for performing kinetic computations [39].

## 3- Results and discussions

Fig. 1 shows the XRD pattern of the as-received melt spun  $\text{Al}_{87}\text{Ni}_{10}\text{La}_3$  alloy. Only a broad peak corresponding to a fully amorphous phase is observed. This confirms that the melt spinning of the alloy was successful to produce the amorphous alloy.

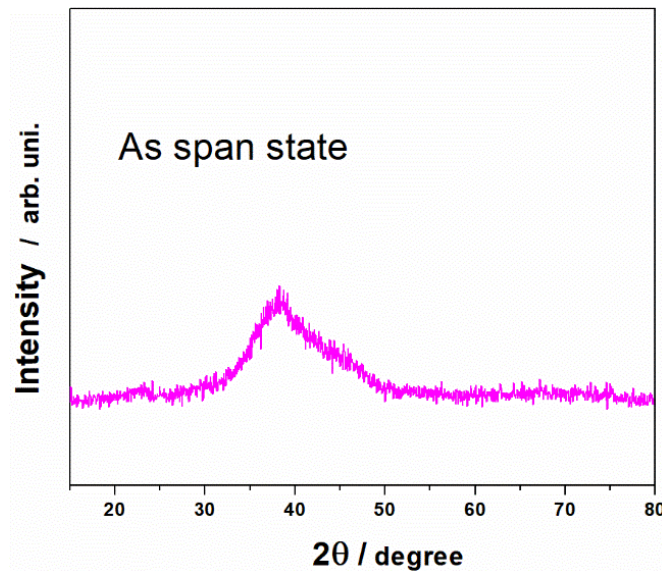


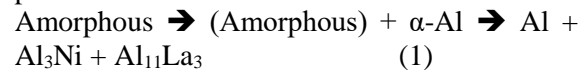
Fig. 1. XRD pattern of  $\text{Al}_{87}\text{Ni}_{10}\text{La}_3$  amorphous alloy.

Fig. 2 shows continuous heating DSC plots for  $\text{Al}_{87}\text{Ni}_{10}\text{La}_3$  amorphous alloy at heating rates of 2.5 to 40 K/min. As it can be seen, the crystallization of the amorphous alloy is a two-stage process and the temperature ranges of these two stages are listed in Table 1.  $T_{x1}$  refers to the onset temperature of the first crystallization stage,  $T_{p1}$  refers to the peak temperature of the first crystallization stage, and so on.

No  $T_g$  is detected prior to the first crystallization onset temperature ( $T_x$ ) either due to weak endothermic peak related to the glass transition temperature or a small fraction of quench-in nuclei that from initially during rapid solidification. These are typical features of crystallization processes in which the primary crystallization of fcc-Al phase occurs [21-23]. The first stage of crystallization for the heating rate of 2.5, 5 and 10 K/min is shown in higher magnification in the Fig.2. Upon increasing the heating rate, all the crystallization peaks shift to higher temperatures indicating a kinetic effect during crystallization of the amorphous alloy and all the peaks become broader. This phenomenon is quite common, and the physical reason has been discussed in the literature [29-34].

Fig. 3 shows the XRD patterns of  $\text{Al}_{87}\text{Ni}_{10}\text{La}_3$  amorphous alloys after heat treatment at 560 K and 650 K. The heat treatment temperature is shown by down arrow in thermal analysis curve of 20 K/min (fig.3-inset). As DSC results show,

the amorphous alloy crystallizes through the primary crystallization of fcc-Al phase from the amorphous matrix in the temperature range of 390–510 K. After the second crystallization peak, XRD patterns are indexed to be  $\text{Al}_3\text{Ni}$  and  $\text{Al}_{11}\text{La}_3$  phases in addition to the equilibrium phase Al. At a higher temperature of 650 K, the alloys are fully crystallized, and the microstructure consists of Al,  $\text{Al}_3\text{Ni}$  and  $\text{Al}_{11}\text{La}_3$  phases. This crystallization process can be presented as below:



The variation of observed temperature peak with applied heating rate can be described by the Kissinger analysis (Eq.(2))[38], or by the Ozawa analysis (Eq. (3)) [39]:

$$\ln\left(\frac{T^2}{\beta}\right) = \frac{E_c}{RT} + A \quad (2)$$

$$\ln(\beta) = -0.4567\left(\frac{E_c}{RT}\right) + B \quad (3)$$

where  $\beta$  is the heating rate,  $R$  is the gas constant,  $E_c$  is apparent activation energy,  $T$  is the peak temperature,  $A$  and  $B$  are constants. The crystallization onset temperatures,  $T_x$ , and the peak temperatures,  $T_{pc}$ , for the two peaks determined from the thermal analysis curves, and the activation energy obtained by Kissinger method are listed in Table 1.

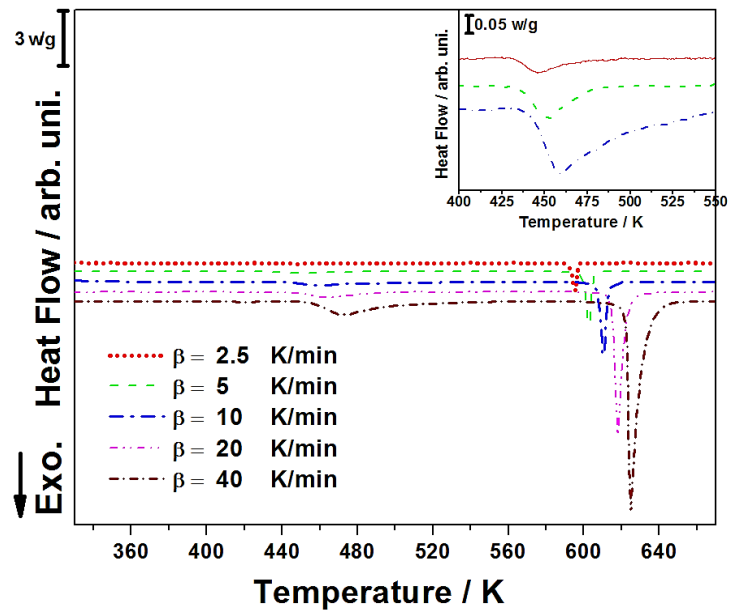


Fig. 2. The STA curves of  $\text{Al}_{87}\text{Ni}_{10}\text{La}_3$  for different heating rates of 2.5, 5, 10, 20 and 40 K/min.

**Table 1.** Characteristic temperatures, apparent activation energy obtained by Kissinger and Ozawa models and change of Avrami index for the primary and secondary crystallization steps of the  $\text{Al}_{87}\text{Ni}_{10}\text{La}_3$  amorphous alloy at different heating rates.

Glass transition	T (K)	Heating rate (K/min)					Activation energy (kJ/mol) ( $\pm 6$ )	
		2.5	5	10	20	40	Kissinger model	Ozawa model
First peak	$T_{x1}$	425	430	430	450	461	175.1	173.7
	$T_{p1}$	445	455	457	462	475		
	Avrami index	1.05	0.96	0.90	0.84	0.81		
Second peak	$T_{x2}$	580	600	610	615	618	282.4	278.4
	$T_{p2}$	597	603	615	618	625		
	Avrami index	4.10	4.05	3.90	3.70	3.50		

$T_{x1}$  and  $T_{x2}$ : onset temperature of the first and second crystallization stage

$T_{p1}$  and  $T_{p2}$ : peak temperature of the first and second crystallization

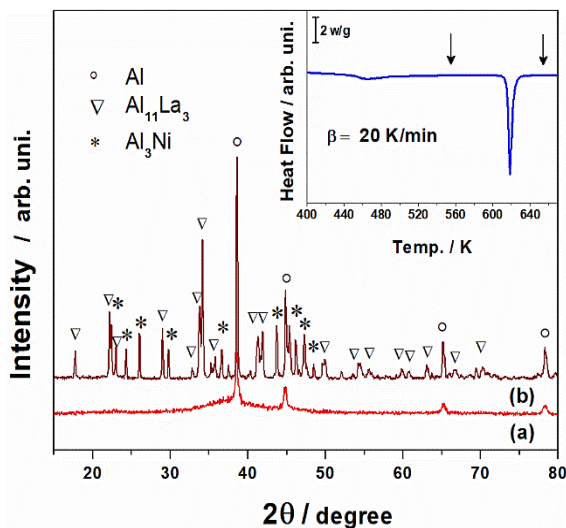


**Fig. 3.** XRD patterns of Al<sub>87</sub>Ni<sub>10</sub>La<sub>3</sub> amorphous alloys after heat treatment at a) 560 K and b) 650 K and thermal analysis curve for heating rate of 20 K/min (inset).

Fig. 4 and Fig. 5 show Ozawa and Kissinger plots. These plots are straight with little scatter, and it could be concluded that in this range of heating rates, there is no change in the reaction mechanism. The apparent activation energies calculated from the gradients of these plots by the Ozawa and Kissinger methods are presented in table 1. As it can be seen, for the first crystallization stage, the apparent activation energy based on the Kissinger model and Ozawa model are about 175.1 and 173.7 kJ/mol, respectively.

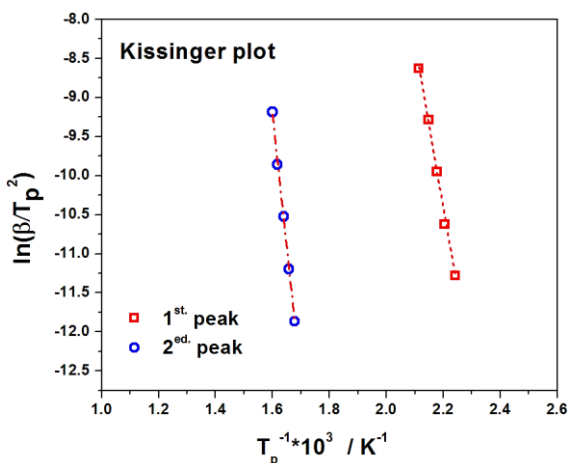


**Fig. 4.** Kissinger plots of crystallization sequences in Al<sub>87</sub>Ni<sub>10</sub>La<sub>3</sub> amorphous alloys for the primary and secondary crystallization steps.

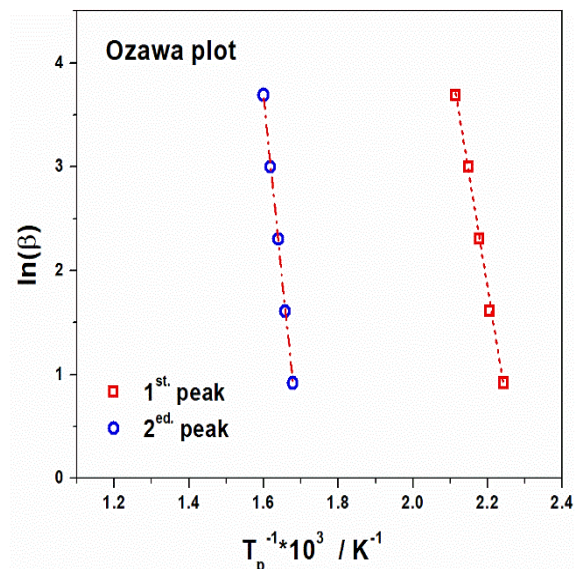


**Fig. 5.** Ozawa plots of crystallization sequences in Al<sub>87</sub>Ni<sub>10</sub>La<sub>3</sub> amorphous alloys for the primary and secondary crystallization steps.

The activation energy of crystallization is a measure of the thermal stability of amorphous alloy. The activation energy of the primary crystallization in this alloy and some other amorphous Al alloys from the literature are listed in Table 2. As indicated in table 2, for the first stage of crystallization of Al-Ni-X amorphous alloys different activation values were reported, which varies from 129- 289 kJ/mol. The obtained activation energy from both models in this study has a value of 175 kJ/mol which is in agreement with other researches. It has been reported that the self-diffusion activation energy of Al, i.e. the activation energy for fcc-Al growth, is 120–140 kJ/mol [40]. Present alloy shows higher activation energy that means an additional energetic cost for the formation of fcc-Al particles due to the formation of Al-La pairs. The presence of La atoms results to decrease in the Al-Al clusters which operate as preferential sites for the nucleation of fcc-Al particles hence more energy is required for the nucleation and formation of fcc-Al particles in Al<sub>87</sub>Ni<sub>10</sub>La<sub>3</sub> amorphous alloy.

**Table 2.** The crystallization activation energy of first peak in the DSC curve for different Al-Ni-X amorphous alloys

No	Composition	E (kJ/mol)	Ref.
1	Al <sub>88</sub> Ni <sub>7</sub> MM <sub>5</sub>	129	41
2	Al <sub>88</sub> Ni <sub>10</sub> MM <sub>2</sub>	140	37
3	Al <sub>87</sub> Ni <sub>10</sub> Ce <sub>3</sub>	181	42
4	Al <sub>87</sub> Ni <sub>10</sub> La <sub>2.1</sub> Ce <sub>2.8</sub> Pr <sub>0.3</sub> Nd <sub>0.6</sub>	217	43
5	Al <sub>87</sub> Ni <sub>8</sub> La <sub>5</sub>	258	41
6	Al <sub>85</sub> Ni <sub>10</sub> Ce <sub>5</sub>	289	44
7	Al <sub>87</sub> Ni <sub>10</sub> La <sub>3</sub>	175	This study

The crystallization activation energies for the second peak calculated by Kissinger and Ozawa model are about 282.4 and 278.4 kJ/mol respectively. Clearly, the activation energy of the second stage of crystallization is higher than the activation energy of first crystallization step because of more complicated crystallization products. As mentioned above, at the second stage of crystallization two new phases of Al<sub>3</sub>Ni and Al<sub>11</sub>La are appeared and need more energy to form. In the process of crystallization, the atoms participating in the crystallization reaction will acquire additional energy to form an activated cluster. The activation energy can be interpreted as the additional energy that an atom must acquire in order to be a part of the activated cluster [45].

The mean value of Avrami index was calculated by Gao-Wang method [46] and the result for the first and second peaks of the thermal analysis curve for different heating rates is presented in Table 1. As it can be seen, this value for the first peak is averagely 0.9 and for the second peak is about 3.8. The Avrami index could be used to determine the crystallization mechanism [47]. Then, for the first crystallization stage of Al<sub>87</sub>Ni<sub>10</sub>La<sub>3</sub> amorphous alloy, the crystallization mechanism is in the diffusion control regime while the second stage is in the interface control regime. This demonstrates that crystallization of Al and the growth of these crystallites requires the rejection of La. The enrichment of La at the interface of crystalline clusters indicates the low mobility of La in the amorphous parent phase. This, in turn, hinders

the growth of the Al nanocrystals. The diffusion of alloying elements in metallic glasses is known to be sensitive to the relative size of the diffusing and the host atoms [48]. The low mobility of La can be explained by its larger atomic radius (0.1879 nm) compared to Ni (0.124 nm) and Al (0.143 nm). Thus, the growth velocity and the final size of the Al crystals are controlled by the diffusion of La into the amorphous matrix. Regions, where La shells around various Al nanocrystals, have merged should be even higher barriers to the growth of these Al crystals.

## Conclusions

Thermal analysis and X-ray diffraction have been employed to investigate the crystallization process in the amorphous Al<sub>87</sub>Ni<sub>10</sub>La<sub>3</sub> alloy. The results demonstrated that the crystallization from amorphous to fully crystalline state consists of two stages. In the first crystallization stage, fcc-Al nanoparticle precipitated from the amorphous matrix while the second crystallization stages is corresponding to the crystallization of Al<sub>3</sub>Ni and Al<sub>11</sub>La<sub>3</sub> phases. The apparent activation energies for the first and second crystallization stages determined by the Kissinger and Ozawa methods. For the first crystallization stage, the apparent activation energy based on the Kissinger model and Ozawa model are about 175.1 and 173.7 kJ/mol, respectively. The crystallization activation energy for the second exothermic peak in thermal analysis curve calculated by Kissinger and Ozawa model are about 282.4 and 278.4 kJ/mol respectively. These values are relatively similar for the different models in each crystallization stage, and these were in agreement with literature. The kinetics investigation showed that the precipitation of fcc-Al phase in first stage took place with decreasing nucleation rate in diffusion control mode, while the second stage was in interface control regime.

## References

- [1] A. Inoue, K. Kohetera, K. Ohtera, A.P. Tsai, T. Masumoto, "Aluminum-Based Amorphous Alloys with Tensile Strength above 980 MPa", J. App. Phys., Vol. 27, 1988, pp.479-482.

- [2] A. Inoue, M. Yamamoto, H. M. Kimura, T. Masumoto, "Ductile aluminium-base amorphous alloys with two separate phases", *J. Mater. Sci. Letter.*, Vol. 6, 1987, pp. 194-196.
- [3] C. Suryanarayana, A. Inoue, *Bulk Metallic Glasses*, 2ed ed., CRC press, Boca Raton, 2011, p.12.
- [4] K.F. Kelton, A.L. Greer, *Nucleation In Condensed Matter Applications In Materials and Biology*, Pergamon series, Pergamone Materials Series, Oxford, 2009, p.14.
- [5] H.H. Lieberman, *Rapidly Solidified Alloys, Processes, Structures, Properties, Applications Materials Engineering*, CRC Press, New York, 1993, p.9.
- [6] J. Sestak, J.J. Mares, P. Hubik, *Glassy, Amorphous and Nano-Crystalline Materials*, Springer Publishing, New York, 2011, p.8.
- [7] M. Tavoosi, M. H. Enayati, F. Karimzadeh, "Formation and crystallization of an amorphous Al<sub>80</sub>Fe<sub>10</sub>Ti<sub>5</sub>Ni<sub>3</sub>B<sub>2</sub> alloy", *Met. Mater. Int.*, Vol. 17, No. 5, 2011, pp. 853-856.
- [8] C.E. Mobley, A.H. Clauer, B. Wilcox, "Microstructures and tensile properties of 7075 aluminum compacted from melt-spun ribbon", *J. Instit. Met.*, Vol. 100, No. 1, 1972, pp. 142-145.
- [9] V. I. Tkatch, A. I. Limanovskii, S. N. Denisenko, S. G. Rassolov, "The effect of the melt-spinning of processing parameters on the rate cooling", *Mater. Sci. Eng. A*, Vol. 323, No. 1, 2002, pp. 91-96.
- [10] L. Katgermana, F. Dom, "Rapidly solidified aluminium alloys by meltspinning", *Mater. Sci. Eng. A*, Vol. 375, No. 1, 2004, pp. 1212-1216.
- [11] E.J. Lavernia, T.S. Srivatsan, "The rapid solidification processing of materials: science, principles, technology, advances, and applications", *J. Mater. Sci.*, Vol. 45, No. 2, 2010, pp. 287-325.
- [12] B. Radiguet, D. Blavette, N. Wanderka, J. Banhart, K.L. Sahoo, "Segregation-controlled nanocrystallization in an Al-Ni-La metallic glass", *App. Phys. Letter.*, Vol. 92, No. 10, 2008, pp. 103126-103128.
- [13] M.C. Gao, G.J. Shiflet, "Devitrification phase transformations in amorphous Al<sub>85</sub>Ni<sub>7</sub>Gd<sub>8</sub> alloy", *Intermetallics*, Vol. 10, No. 11-12, 2002, pp. 1131-1139.
- [14] D. Jacovkis, J. Rodriguez-Viejo, M.T. Clavaguera-Mora, "Isokinetic analysis of nanocrystallization in an Al-Nd-Ni amorphous alloy", *J. Phys. Cond. Mater*, Vol. 17, No. 32, 2005, pp. 4897-4910.
- [15] F. Sun, T. Gloriant, "Primary crystallization process of amorphous Al<sub>88</sub>Ni<sub>6</sub>Sm<sub>6</sub> alloy investigated by differential scanning calorimetry and by electrical resistivity", *J. Alloy. Compd.*, Vol. 477, No. 1, 2009, pp. 133-138.
- [16] M. Salehi, S.G. Shabestari, S.M.A. Boutorabi, "Nano-crystal development and thermal stability of amorphous Al-Ni-Y-Ce alloy", *J. Non-cryst. Solid.*, Vol. 375, 2013, pp.7-12.
- [17] A. Inoue, K. Nakazato, Y. Kawamura, A.P. Tsai, T. Masumoto, "Effect of Cu or Ag on the Formation of Coexistent Nanoscale Al Particles in Al-Ni-M-Ce (M=Cu or Ag) Amorphous Alloys", *Mater. Trans.*, Vol. 35, No. 2, 1994, pp. 95-102.
- [18] K. Song, Xi. Bian, J. Guo, Xu. Li, M. Xie, Ch. Dong, "Study of non-isothermal primary crystallization kinetics of Al<sub>84</sub>Ni<sub>12</sub>Zr<sub>1</sub>Pr<sub>3</sub> amorphous alloy", *J. Alloy. Compd.*, Vol. 465, No. 1-2, 2008, pp. 7-13.
- [19] S.-H. Wang, X.-F. Bian, H.-R. Wang, "crystallization of amorphous Al<sub>84.2</sub>Ni<sub>10</sub>La<sub>2.1</sub>Ce<sub>2.8</sub>Pr<sub>0.3</sub>Nd<sub>0.6</sub> alloy", *Mater. Letter.*, Vol. 58, No. 1, 2004, pp. 539-542.
- [20] A.K. Gangopadhyay, T.K. Croat, K.F. Kelton, "The effect of phase separation on subsequent crystallization in Al<sub>88</sub>Gd<sub>6</sub>La<sub>2</sub>Ni<sub>4</sub>", *Acta Mater.*, Vol. 48, No. 16, 2000, pp. 4035-4043.
- [21] M. Tavoosi, M. H. Enayati and F. Karimzadeh, "Crystallisation process of Al<sub>80</sub>Fe<sub>10</sub>Ti<sub>10</sub> amorphous phase",

- Powd. Metal., Vol. 54, No. 3, 2011, pp. 445-449.
- [22] J. Antonowicz, "Phase separation and nanocrystal formation in Al-based metallic glasses", *J. Alloy. Compd.*, Vol. 434-435, No. 1, 2007, pp. 126-130.
- [23] R.I. Wu, G. Wilde, J.H. Perepezko, "Glass formation and primary nanocrystallization in Al-base metallic glasses", *Mater. Sci. Eng. A*, Vol. 301, No. 1, 2001, pp. 12-17.
- [24] J. Antonowicz, "Atomic packing and phase separation in Al-rare earth metallic glasses", *J. Mater. Sci.*, Vol. 45, No. 18, 2010, pp. 5040-5044.
- [25] J. Antonowicz, M. Kędzierski, E. Jezierska, J. Latuch, A.R. Yavari, L. Greer, P. Panine, M. Sztucki, "Small-angle X-ray scattering from phase-separating amorphous metallic alloys undergoing nanocrystallization", *J. Alloy. Compd.*, Vol. 483, No. 1, 2009, pp. 116-119.
- [26] J. Antonowicz, A.R. Yavari, W.J. Botta, P. Panine, "Phase separation and nanocrystallization in Al<sub>92</sub>Sm<sub>8</sub> metallic glass", *Philosophical Mag.*, Vol. 86, No. 27, 2006, pp. 4235-4242.
- [27] N. Tian, M. Ohnuma, T. Ohkubo, K. Hono, "Primary Crystallization of an Al<sub>88</sub>Gd<sub>6</sub>Er<sub>2</sub>Ni<sub>4</sub> Metallic Glass", *Mater. Trans.*, Vol. 46, No. 12, 2005, pp. 2880-2885.
- [28] H.E. Kissinger, *J. Res.*, "Variation of peak temperature with heating rate in differential thermal analysis", *J. Res. Nation. Bureau Stand.*, Vol. 57, No. 1, 1956, pp. 217-221.
- [29] H.E. Kissinger, "Reaction kinetics in differential thermal analysis," *Analy. Chem.*, Vol. 29, No. 1, 1957, pp. 1702-1706.
- [30] G. Wilde, H. Sieber, J.H. Perepezko, "Glass formation in Al-rich Al-Sm alloys during solid state processing at ambient temperature", *J. Non-Cryst. Solid.*, Vol. 250, 1999, pp.621-625.
- [31] E. Illekova, K. Czomorova, F.A. Kuhnast, J.M. Fiorani, "Transformation kinetics of the Fe<sub>73.5</sub>Cu<sub>1</sub>Nb<sub>3</sub>Si<sub>13.5</sub>B<sub>9</sub> ribbons to the nanocrystalline state", *Mater. Sci. Eng. A*, Vol. 205, 1996, pp.166-179.
- [32] W.Z. Chen, P.L. Ryder, "X-ray and differential scanning calorimetry study of the crystallization of amorphous Fe<sub>73.5</sub> Cu<sub>1</sub>Nb<sub>3</sub> Si<sub>13.5</sub>B<sub>9</sub> alloy", *Mater. Sci. Eng. B*, Vol. 34, 1995, pp. 204-209.
- [33] S.D. Kaloshkin, I.A. Tomilin, "The crystallization kinetics of amorphous alloys. *Thermochimica Acta*, Vol. 280-281, 1996, pp. 303-317.
- [34] D. Crespo, T. Pradell, M.T. Clavaguera-Mora, N. Clavaguera, "Microstructural evaluation of primary crystallization with diffusion-controlled grain growth", *Phys. Rev. B*, Vol. 55, 1997, pp. 3435-3444.
- [35] H. Matyja, T. Kulik, A. Conde, C.F. Conde, M. Millan (Eds.), *Trends in Non-crystalline Solids*, World Scientific, Singapore, 1992, p.124.
- [36] J.M. Barandiaran, I. Teller, J.S. Garitaonandia, H.A. Davies, "Kinetic aspects of nano-crystallization in Finemet-like alloys. *J. Non-Cryst. Solid*, Vol. 329, 2003, pp. 57-62.
- [37] M. Mansouri, A. Simchi, N. Varahram, E.S. Park, "Development of fcc-Al nanoparticles during crystallization of amorphous Al-Ni alloys containing mischmetal: Microstructure and hardness evaluation", *Mater. Sci. Eng. A*, Vol. 604, 2014, pp. 92-97.
- [38] S. Vyazovkin, K. Chrissafis, M.L.D. Lorenzo, N. Koga, M. Pijolat, B. Roduit, N. Sbirrazzuoli, J.J. Suñol, "ICTAC Kinetics Committee recommendations for collecting experimental thermal analysis data for kinetic computations", *Thermochim. Acta*. Vol. 590, 2014, pp.1-23.
- [39] S. Vyazovkin, A.K. Burnham, J.M. Criado, L.A. Pérez-Maqueda, C. Popescu, N. Sbirrazzuoli, "ICTAC Kinetics Committee recommendations for performing kinetic computations on thermal analysis data", *Thermochim. Acta*, Vol. 520, 2011, pp.1-19.



- [40] Y. Khan, M. Sostarich, "Dynamic temperature X-ray diffraction analysis of amorphous Fe<sub>80</sub>B<sub>20</sub>", *Zeitschrift Fur Metallkunde*, Vol.72, 1981, pp. 266-268.
- [41] G. Abrosimova, A. Aronin, V. Stelmukh, "Crystallization of amorphous Fe<sub>85</sub>B<sub>15</sub> above glass transition temperature", *Solid State Phys.*, Vol. 33, 1991, pp. 3570-3576.
- [42] I.G. Brodova, I.G. Shirinkina, O.A. Antonova, E.V. Shorokhov, I.I. Zhgilev, "Formation of a submicrocrystalline structure upon dynamic strain of aluminum alloys", *Mater. Sci. Eng. A*, Vol. 503, 2009, pp.103-105.
- [43] T. Masumoto, R. Maddin, "Structural stability and mechanical properties of amorphous metals", *Mater. Sci. Eng. A*, Vol. 19, 1975, pp. 1-24.
- [44] G. Abrosimova, A. Aronin, D. Matveev, E. Pershina, "Nanocrystal formation, structure and magnetic properties of Fe-Si-B amorphous alloy after strain", *Mater. Letter.*, Vol. 97, 2013, pp.15-17.
- [45] A. Aronin, D. Matveev, E. Pershina, V. Tkatch, G. Abrosimova, "The effect of changes in Al-based amorphous phase structure on structure forming upon crystallization", *J. Alloy. Compd.*, Vol. 715, 2017, pp.176-183
- [46] Y.Q. Gao, W. Wang, "On the activation energy of crystallization in metallic glasses", *J. Non-Cryst. Solids*, Vol. 81, 1986, pp. 129–134.
- [47] T. Ozawa, "Kinetic analysis of derivative curves in thermal analysis", *J. Thermal Analy.*, Vol. 2, 1970, pp. 301–324.
- [48] F. Faupel, W. Frank, M.-P. Macht, H. Mehrer, V. Naundorf, K. Rätzke, H. Schober, S. Sharma, H. Teichler, "Diffusion in metallic glasses and supercooled melts", *Rev. a.*, Vol. 75, No.1, 2003, pp. 237-280.